International Journal of Physical Sciences Vol. 7(14), pp. 2166 - 2173, 30 March, 2012
Available online at http://www.academicjournals.org/IJPS
DOI: 10.5897/IJPS12.024
ISSN 1992 - 1950 ©2012 Academic Journals

Full Length Research Paper

Application of Pt-Rh complex catalyst: Feasibility study on the removal of gaseous ammonia

Chang-Mao Hung

Department of Vehicle Engineering, Yung-Ta Institute of Technology and Commerce, 316 Chung-Shan Road, Linlo, Pingtung 909, Taiwan, Republic of China. E-mail: hungcm1031@gmail.com. Tel: +886-8-7233733/508. Fax: +886-8-7228046.

Accepted 19 March, 2012

The selective catalytic oxidation (SCO) of gas phase ammonia (NH_3) to nitrogen and water has been proposed as an effective ammonia removal process. This study reports that the oxidation of NH_3 with oxygen to form N_2 was investigated by SCO using a Pt-Rh complex catalyst that was synthesized by the incipient wetness impregnation process. The catalysts were performed using fluorescent spectroscopy (FS) combined with UV-Vis absorption, cyclic voltammetry (CV), linear sweep voltammograms (LSV), zeta potential measurements and dynamic light-scattering (DLS). The findings show that the ammonia removal by catalytic oxidation over the Pt-Rh complex catalyst was nearly 95% at a temperature of 623K and an oxygen content of 4%. N_2 was the main end product of the NH_3-SCO process. FS have been applied to evaluate the catalyst yields with fluorescent peaks of 270 and 390 nm at room temperature. These results suggest that FS was proven to be an appropriate and effective method to characterize the Rh clusters that enhance their intrinsic emission from Pt-Rh complex catalyst in catalytic treatment systems. The CV and LSV reversible redox ability may explain the significant activity of the catalysts.

Key words: Selective catalytic oxidation (SCO), ammonia (NH_3), Pt-Rh complex catalyst, fluorescent spectroscopy (FS), cyclic voltammetry (CV), linear sweep voltammograms (LSV).

INTRODUCTION

Ammonia nitrogen is a common environmental prominent problems that are emitted by a number of various sources, including urea manufacturing, nitrogen fertilizer production, gasification biomass and coal, petroleum refining and refrigeration, livestock waste and agriculture activities. Ammonia (NH_3) is a common, corrosive and highly toxic and reactive inorganic gas with a pungent odor under ambient conditions and has recently been described to be potentially damaging to health and the ecosystem concerns (Hung, 2007; Galloway et al., 2008; Zhang et al., 2010; Hung et al., 2010; Birch et al., 2011; Hung, 2011a). More and more attention has been given to the removal of NH_3 from gaseous and waste streams and the control of NH_3 emissions are important all over the world. It is known to be a variety of approaches that have been developed by the previous investigator to treat NH_3 biologically, physically and chemically, such as using conventional biological nitrification, breakpoint chlorinate-ion, air stripping, ion-exchange, scrubbing with water, using post-combustion control, adsorption by activated carbon, etc., all of which cause a phase transformation and may yield contaminated sludge or adsorbent, which must be further treatment with the strict discharge requirements.

Among these, the most widely used an attractive alternative approach for solving the NH_3-containing gas pollution is the selective catalytic oxidation (SCO) of ammonia (SCO-NH_3) into nitrogen gas and water, as reported elsewhere (Cui et al., 2010; Hung, 2011b). To date, development of this technology is an important heterogeneous catalytic process that has attracted significant attentions, and increases the effectiveness of the oxidation process by using certain catalysts, which potentially shorten the reaction time of the oxidation and allow the reaction to proceed under stable operating conditions. The SCO-NH_3 process should be selective for nitrogen and should prevent further oxidation of nitrogen. Several papers published some results of various compositions of catalysts applied to oxidize gaseous NH_3. For example, Scott and Leech (1927) reported that the

catalytic conversion of NH_3 over a Co-Bi and Co-Al catalyst at 1073K in the catalysis oxidation reaction. Schmidt-Szałowski et al. (1998) proposed a hypothetical mechanism of the effect of these catalysts, their activity and their selectivity in oxidizing NH_3. A study by Wang et al. (1999) investigated the Ni-based catalysts for oxidizing the fuel gas that is produced by the gasification of biomass and found that fresh Ni-based catalysts were more active at lower temperatures in the decomposition of NH_3 and that the partial pressure of hydrogen in the flue gas determined the extent of NH_3 oxidation. Amblard et al. (2000) performed excellent selective conversion of NH_3 to N_2 using a γ-Al_2O_3-supported Ni catalyst in an SCO process. The activation of surface NH_x to be the rate limiting step was also noticed. Liang et al. (2000) examined the oxidation of NH_3 in a fixed-bed micro-reactor in a temperature range of 873 to 1023K at a gas hourly space velocity (GHSV) of 1800 to 3600 h^{-1} and found that the conversion of NH_3 reached 98.7 and 99.8% on nitrided MoNx/α-Al_2O_3 and NiMoNy/α-Al_2O_3 catalysts, respectively. Hung (2008) described the catalytic oxidation of NH_3 in a gaseous stream using a nanoscale copper-cerium bimetallic catalyst in a temperature range of 423 to 673K at a GHSV of 92,000 h^{-1}. The bimetallic nanoscale structure had the greatest NH_3 reduction activity, and the N_2 selectivity exhibited a synergistic effect. Hence, this study indicates that the SCO-NH_3 process was suitable for catalytic oxidation of NH_3. Recently, Zhang et al. (2009) demonstrated the excellent selective conversion of NH_3 to gaseous nitrogen over an Ag-Al_2O_3 catalyst at 413K in an SCO process. Brüggemann and Keil (2009) developed a density functional theory of the effect of H-ZSM-5 catalysts and their activity and selectivity in oxidizing NH_3. Biausque and Schuurman (2010) studied the catalytic oxidation of NH_3 to NO in a gaseous stream using a $LaCoO_3$ catalyst and found out that the NO and N_2O are formed through parallel routes from NH_3 via surface nitroxyl species. Moreover, the kinetic behavior of NH_3 oxidation with catalysis can be accounted by using the rate expression of the Mars and Van Krevelen type kinetic model.

In general, platinum-based metal additives, used as three-way catalysts and electrocatalysts, due to their selective catalytic and oxidation-reduction potential (ORP) properties are the most active components in hydro-carbon oxidation, and are also active in methanol fuel cells electro-oxidation reactions based on these functional materials (Choi et al., 2004). The use of rhodium-based metal improves the nitrogen oxide conversion properties of the catalysts, including selectivity towards dinitrogen; it also reduces poisoning by carbon monoxide (Stoyanovskii et al., 2009). Normal operating conditions are well within the ranges of stability of platinum and rhodium and of the components that are used to stabilize the surface area of the catalyst (Zhang and Geddes, 2010). More importantly, limited studies have investigated the use of the Pt-Rh complex material in the catalytic gaseous-phase oxidation of NH_3. As a result, the present investigation was conducted to evaluate the activity of the Pt-Rh complex catalyst in the oxidation of NH_3 under various conditions and the effect of this catalyst on the decomposition of NH_3 in SCO processes. In this context, the excitation fluorescence spectroscopy was used as an effective tool across a range of excitation and emission wavelengths for under-standing information regarding catalyst characteristics during catalytic process. Hence, the catalysts were characterized by fluorescent spectroscopy (FS), UV-Vis absorption, cyclic voltammetry (CV), linear sweep voltammograms (LSV), zeta potential and dynamic light-scattering (DLS).

MATERIALS AND METHODS

Chemicals

The Pt-Rh complex catalysts that were used in this work were prepared by the incipient wetness impregnation method with aqueous H_2PtCl_6 and $Rh(NO_3)_3$ (all grade, Merck, Darmstadt, Germany). The precipitate was washed with distilled water and then dried at 573K for 8 h. The Pt-Rh complex catalyst, with a Pt to Rh weight ratio of 5 to 1, was wash-coated on a γ-Al_2O_3 substrate with a constant active metals ratio of 4.4%. The catalysts were then calcined at 873K in an air stream for 6 h. The resulting powder was formed into tablets using acetic acid as a binder. The tablets were later reheated at 673K to burn off the binder and then crushed and sieved into various particle sizes ranging from 0.25 to 0.15 mm.

Experimental set up

These experiments were conducted in a tubular fixed-bed quartz reactor (TFBR). The typical reactant gas, which flowed into the inlet of the reactor (GHSV, 92,000 h^{-1}), composed of 600 ppm NH_3, 4% O_2 and He. A mass flow regulator was used to independently control the flows of NH_3 and O_2. Highly pure He was used as a carrier gas at a flow rate ranging from 8 to 13 L/min and was controlled using a mass flow meter (830 Series Side-Trak™, Sierra, Monterey, CA, USA). This approach resembled that of Hung (2008), who conducted experiments on the catalytic oxidation of NH_3. A reaction tube with a length of 300 mm and an inner diameter of 28 mm was placed inside a split tube furnace with the tube that contained the catalyst. The temperature was measured using two type-K thermocouples (KT-110, Kirter, Kaohsiung, Taiwan), each with a diameter of 0.5 mm, located in front of and behind the catalytic bed. The thermocouples were also connected to a proportional integral derivative (PID) controller (FP21, Shimaaen, Tokyo, Japan) to maintain the temperature in the tube within ± 0.5%.

Analytical methods

Before and after the reaction, the samples were automatically injected through a sampling valve into a gas chromatograph (Shimadzu GC-14A), equipped with a thermal conductivity detector. A stainless-steel column (Porapak Q 80/100 mesh) was used to separate the components of the gas and determine the concentration of N_2O isothermally at 100°C. The areas associated with the signals were electronically measured using a data integrator (CR-6A, Shimadzu, Kyoto, Japan). Dilute sulfuric acid was used to scrub the residual NH_3 in the vapor gas, and the amount of NH_3 was measured using a Merck kit (Merck, Spectroquant Pharo 300, Darmstadt, Germany). The concentrations

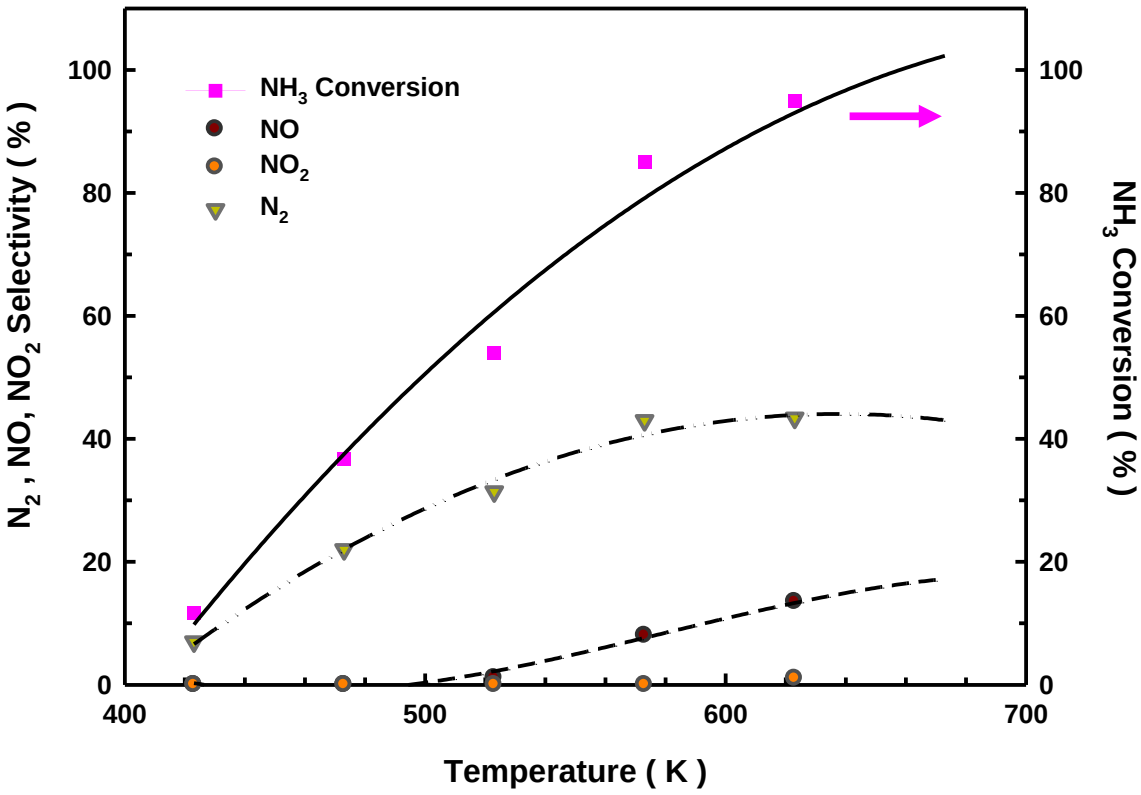

Figure 1. Relationship of the ammonia conversion, N_2, NO and NO_2 yield at various temperatures over the Pt-Rh complex catalyst. Test conditions: 600 ppm NH_3 in He, O_2 = 4%, R.H. = 12%, Temperature = 423-623K, GHSV = 92000 ml/h-g.

of NO, NO_2 and O_2 in the gas samples were monitored continuously during the reaction at a particular location in the reactor, using a portable flue gas analyzer (IMR-3000, Neckarsulm, Germany). Data were collected after the SCO reaction had reached steady-state, typically after 20 min at each temperature. Each temperature was maintained for 90 min to allow the system to reach steady-state. Most experiments were repeated once to ensure reproducibility, and similar results were always obtained.

Fluorescence spectroscopy (FS) can be adopted to provide a complete spectral characterization of catalyst material. In this work, fluorescent spectra were obtained using a luminescence spectrophotometer (F-4500, Hitachi, Japan) with a xenon lamp as the excitation source. The emission spectra are plotted on the x-axis, while the excitation spectra are potted parallel to the y-axis. The widths of all slits at both the excitation and emission monochromators were 10 nm. In this investigation, fluorescent spectra comprised 60 excitation and 60 emission spectra from 200 to 800 nm, yielding discrete values of fluorescence intensity at 3600 excitation/emission wavelength pairs. Spectral subtraction was performed to remove the blank spectra from pure water. UV-Vis absorption spectra of the solid sample were obtained using a photo spectrophotometer (U-2900, Hitachi, Japan). Cyclic voltammetry (CV) and linear sweep voltammograms (LSV) measurements were conducted at room temperature with an electrochemical analyzer (CHI 6081D, USA) using a three-electrode electrochemical cell to investigate the oxidation/reduction of the powder samples. The working electrode (WE) was a glassy carbon electrode, and the samples were scanned at a rate of 10 mV/s with the potential cycled between -0.2 and 1.2 V. The counter electrode (CE) was a platinum wire, and a saturated hydrogen electrode (SHE) was employed as the reference electrode (RE). H_2SO_4 (0.5 M) was used as the electrolyte solution. A zeta potential analyzer (Zetasizer 2000HAS, Malvern, UK) was used to perform the particle size and the zeta potential determination.

RESULTS AND DISCUSSION

Product selectivity

First, the experimental results show that the NH_3-SCO method is effective for the catalytic of NH_3. Thus, it can be observed from Figure 1 that the overall selectivity of N_2 production was 7 to 42%, and that of NO production was 0 to 18% over the range of 13 to 95% NH_3 conversion at NH_3 concentrations of 600 ppm. It can be seen that Pt-Rh complex is very active for NH_3 oxidation and shows high conversion even below 473K. It is noteworthy that nitrogen gas was formed primarily by direct dissociation of the NO produced by oxidation of adsorbed NH_3 (Hu et al., 1998; Biausque and Schuurman, 2010). Therefore, NH_3 and oxygen were adsorbed onto specific sites on the Pt-Rh complex catalyst, promoting rapid conversion of NH_3 to nitrogen and water. Moreover, the Pt-Rh complex likely play an important role in the catalytic oxidation of NH_3, and

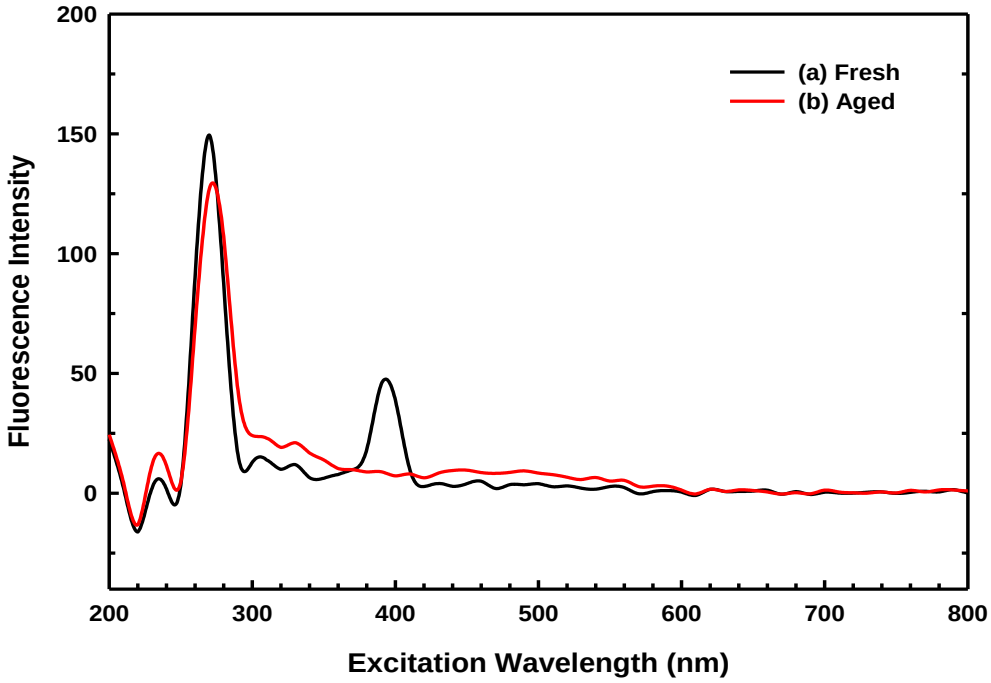

Figure 2. The fluorescent spectra of (a) fresh and (b) after activity test Pt-Rh complex catalyst. Test conditions: 600 ppm NH_3 in He, O_2 = 4%, GHSV = 92000 h^{-1}.

alumina may only offer active sites for the reaction during a catalyzed oxidation run. Furthermore, catalytic activity may be caused by a strong interaction between the Pt-Rh complex and alumina. An earlier work revealed that Rh_2O_3 is the most active phase in the catalytic reaction, because it is a good promoter of oxygen storage and exhibits selectivity towards dinitrogen, thereby promoting NH_3 decomposition. However, some noble metals have been used as catalysts in this process (Mulukutla et al., 2002). The rhodium dioxide in a platinum catalyst may be assumed to promote the formation of the active phase of PtO_2 upon the oxidation of ammonia. Consequently, nitrogen was the dominant gas, and a small amount of NO was detected in the resultant stream. These results indicate that when gaseous oxygen is fed into the reactor with NH_3, the oxidation of NH_3 becomes an unimportant step in the reaction. The oxidation of NH_3 to N_2 may be the first step in the interaction of NH_3 with excess oxygen. The availability of oxygen on the surface lattice is normally considered to be an essential property of oxide catalysts for selective oxidation (Curtin et al., 2000). Apparently, the NH_3-SCO reaction mechanism should be selective toward nitrogen and prevent its further oxidation.

Physico-chemical characterization of the Pt-Rh complex catalyst

At the next step, to further elucidate the reactive property of catalyst in this work, using excitation plot position from the fluorescent spectrometer can generate effective data for characterizing the properties of catalyst. Figure 2a displays the fluorescent spectra for fresh Pt-Rh complex catalyst; two significant excitation peaks at 270 and 390 nm were observed. The fluorescent spectra of Pt-Rh complex catalyst after activity test as shown in Figure 2b was obvious; the significant excitation peaks at 280 nm, were observed. These excitation peaks of the catalyst can be described as metal-enhanced fluorescence (MEF) effect, in which the fluorescence is associated with the Rh clusters of the Pt-Rh complex catalyst surface sites during the reaction. This result is similar to that of Zhang et al. (2010), who found the fluorescence wavelength of 10 nm Rh nanoparticles at 200 to 300 nm.

To further identify the chemical properties of the Pt-Rh complex catalyst, Figure 3 presents UV-Vis absorption spectra and thus provides further information on the states of platinum and rhodium species in these catalysts. The bands associated with such platinum particles were observed at 230 nm (Wu and Lai, 2004). No rhodium-containing species are detected by UV-Vis. These results indicate that rhodium may exist in a highly dispersed form.

In order to provide additional information on the properties of the Pt-Rh complex catalyst, experiments were conducted with the CV profiles of the fresh and aged Pt-Rh complex catalyst. The CV plots reveal that the fresh Pt-Rh complex catalyst has a greater reversible redox capacity than the aged Pt-Rh complex catalyst, with

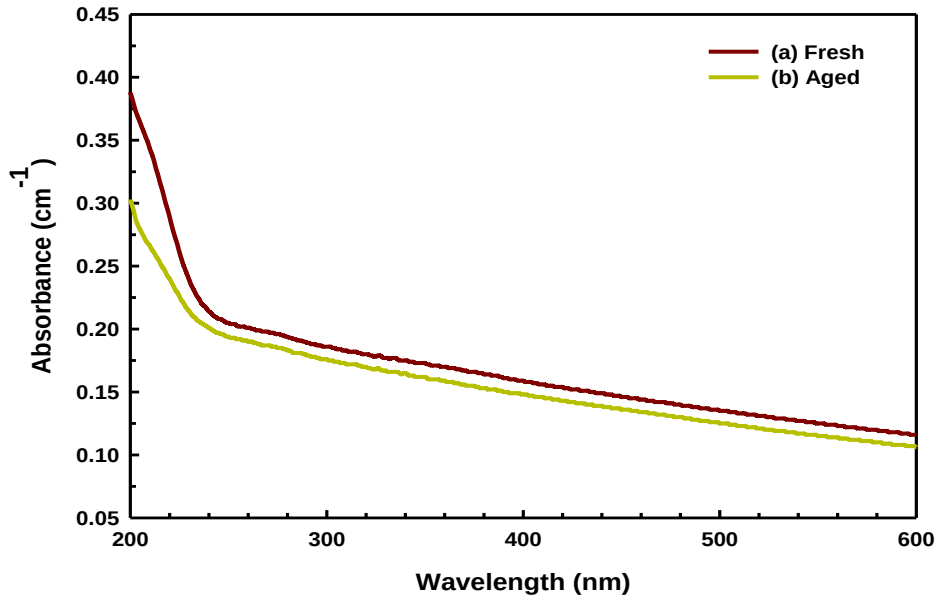

Figure 3. UV-Vis absorption spectra of the Pt-Rh complex catalyst (a) before and (b) after the activity test. Test conditions: 600 ppm NH_3 in He, O_2 = 4%, RH = 12%, GHSV = 92000 h^{-1}.

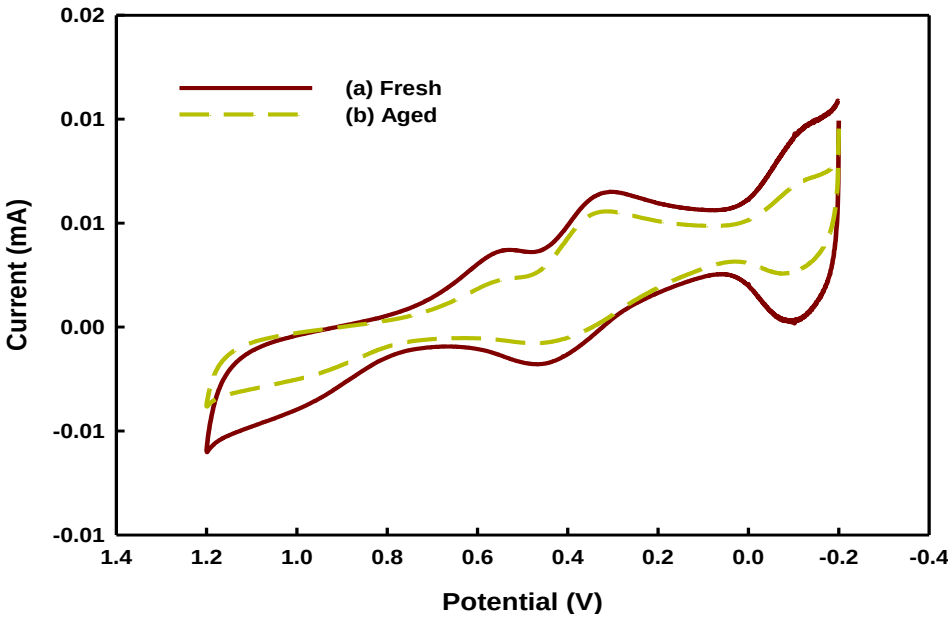

Figure 4. Cyclic voltammograms of the Pt-Rh complex catalyst (a) before and (b) after the activity test in a 0.5 M H_2SO_4 electrolyte solution recorded at a scan rate of 10 mV/s.

with well marked oxidation peaks at 0.5 and 0.3 V (Figure 4). This reversible redox ability may explain the significant activity of the catalysts. An earlier investigation demonstrated that Rh_2O_3 is the most active phase in the catalytic reaction, because it is a strong promoter of oxygen storage (Prasad and Chavdhari, 1994). When it is present in a platinum catalyst, it can be assumed to promote the formation of the active phase of PtO during NH_3 oxidation. The catalytic activity of the Pt-Rh complex catalyst system in the oxidation of NH_3 is explained by the storage and release of O_2 by the oxygen buffers, because the $Rh^{3+} - Rh^0$ redox couple produces oxygen vacancies and increases oxygen mobility, promoting the bifunctional mechanism of the catalyst. Furthermore, the

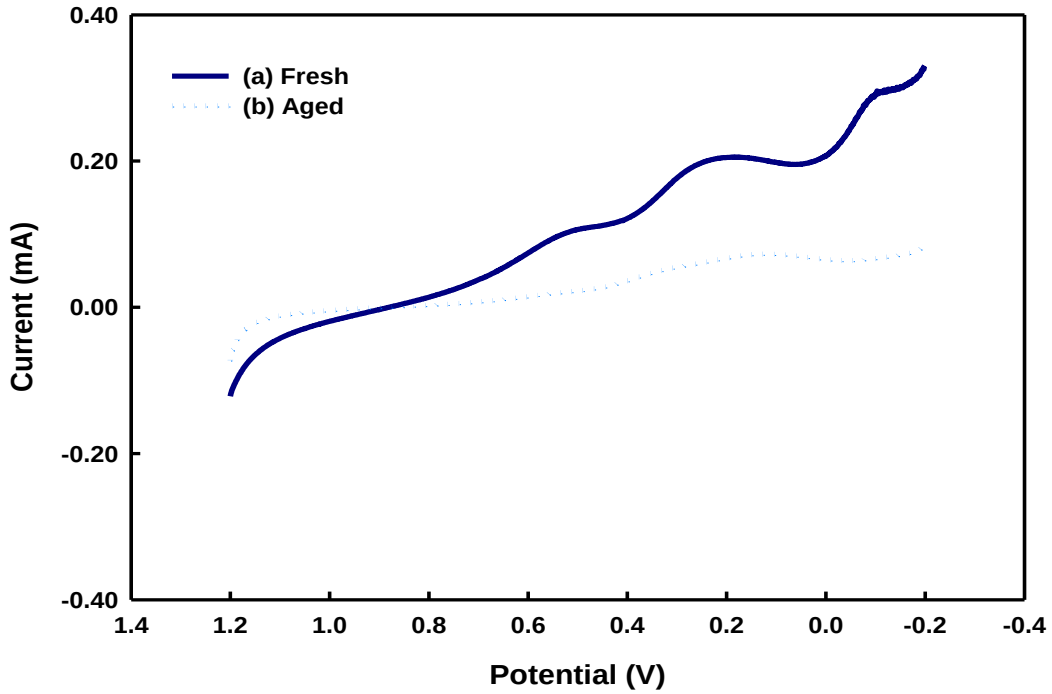

Figure 5. Linear sweep voltammograms of the Pt-Rh complex catalyst (a) before and (b) after the activity test in a 0.5 M H_2SO_4 electrolyte solution recorded at a scan rate of 10 mV/s.

generation of rhodium hydroxide species ($Rh(OH)_x$) was measured with reduction peaks at 0.5 V (Oliveira et al., 2008). Therefore, NH_3 is believed to have adsorbed on the surface of the catalyst before undergoing an oxidation-reduction reaction on the platinum and rhodium oxide active sites.

Figure 5 also shows the electrochemical behavior of LSV profiles of the fresh and aged Pt-Rh complex catalyst. A rapid rise in current density did not appear until about 0.7 V was observed. Furthermore, the LSV plots reveal that the fresh Pt-Rh complex catalyst has a greater reversible redox capacity and oxidation current density than does the aged Pt-Rh complex catalyst, with shoulder around 0.2 and -0.1 V, respectively. Particularly, this reversible redox ability may explain the significant activity of the catalysts. In contrast, the aged Pt-Rh complex catalyst gives negligible oxidation-reduction current in this potential window.

Zeta potential and particle size are important elements for the characterization and applied for catalyst materials research. Figure 6 displays the zeta potential of the fresh and used catalysts and demonstrates that the catalyst changed during exposure to the catalytic oxidation environment. The results reveal that the particle mean zeta potential converged to 7.59 mV for fresh Pt-Rh complex catalyst. However, the zeta potential of the catalyst declined after activity test and the particle mean zeta potential was around -22.6 mV, indicating that catalyst particle zeta potential effect complicated by weak electrostatic repulsion of the solid particle surface charge mechanism and there is tendency to flocculate after catalytic reaction (Du et al., 2008). Obviously, this understanding agrees with the previous observation of the particle size associated with catalyst. Hence, such changes in the zeta potential of the catalyst can be attributed to the colloidal particles that became unstable for the Pt-Rh complex catalyst surface sites during the reaction. The zeta potential that may be dependence of different pH value to this platinum-based composite material will be studied in the future.

Finally, to assess the change in the sizes of particles of the catalyst was determined using the dynamic light-scattering (DLS) method, as shown in Figure 7. The mean particle size converged to approximately 353 nm for fresh Pt-Rh complex catalyst. However, the diameters of the catalyst increased after activity test and the mean particle size was around 729 nm, indicating that catalyst due to the absence of agglomeration or aggregation and the particle size effect complicated by particle migration, sintering and coalescence mechanism after catalytic reaction (Prasad and Chavdhari, 1994). There also appears to be a narrow size distribution with the Pt-Rh particles. Hence, such changes in the sizes of particles of the catalyst can be attributed to over-oxidation of the Pt-Rh complex catalyst surface sites during the reaction.

Conclusions

This study evaluated the Pt-Rh complex catalysts in the

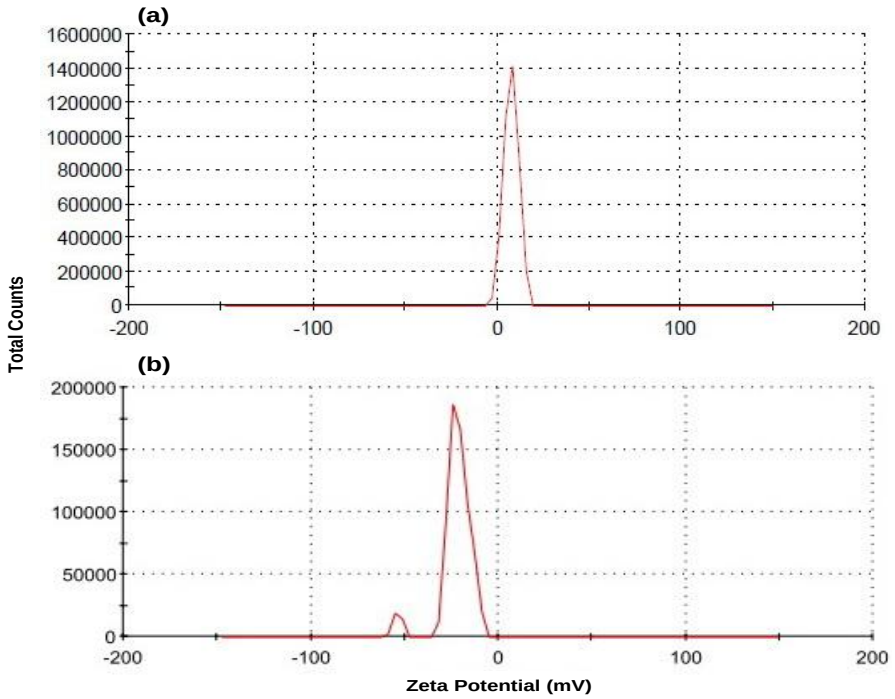

Figure 6. Change in the zeta potential of the Pt-Rh complex catalyst (a) before and (b) after the activity test. Test conditions: 600 ppm NH_3 in He, O_2 = 4%, GHSV = 92,000 h^{-1}.

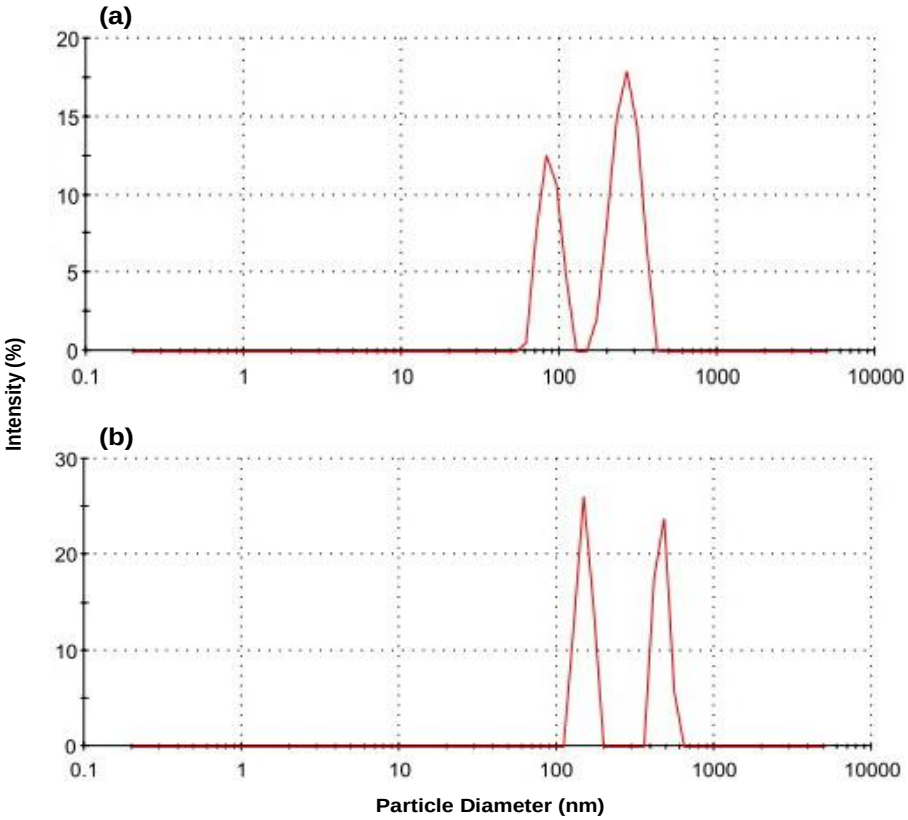

Figure 7. Change in the particle size distributions of the Pt-Rh complex catalyst (a) before and (b) after the activity test. Test conditions: 600 ppm NH_3 in He, O_2 = 4%, GHSV = 92,000 h^{-1}.

SCO-NH_3 reaction of the NH_3 catalytic to form nitrogen as promising and effective as the other treatment methods. Also, Pt-Rh complex catalysts were successfully synthesized and characterized. Results showed that at optimum conditions for the overall selectivity of the NO by-product varied from 0 to 18%, and the N_2 production varied from 7 to 42% with a 13 to 95% NH_3 conversion at 623K when a Pt-Rh complex catalyst was used. Additionally, the experimental results indicate that the SCO-NH_3 process is reasonably selective for nitrogen and may prevent its further oxidation. Moreover, according to a fluorescent spectrometry evaluation, fresh Pt-Rh complex catalyst yielded fluorescent peaks at 270 and 390 nm. This can make excitation fluorescent spectra a nondestructive and sensitivity technique for developing modality for the fluorescent species detection of catalyst complexes. An electrochemical characterization has been performed and reveals that the reversible redox ability may explain the significant activity of the catalysts based on the CV and LSV over a wide potential range. The particle size and zeta potential of the catalyst were determined in the catalytic process. In SCO-NH_3 process, the Pt-Rh complex catalyst performs remarkably well in the treatment of highly concentrated streams of NH_3 and may therefore lead to improvement of industrial plants to meet increasingly stringent regulations concerning NH_3 discharge and addresses environmental sustainability in this field.

ACKNOWLEDGEMENTS

The authors would like to thank the National Science Council of the Republic of China, Taiwan for financially supporting this research under Contract Number NSC 98-2221-E-132-003-MY3. The author thanks Prof. W. L. Lai, in the Department of Environmental Science and Occupational Safety and Hygiene at Tajen University of Science and Technology, for his support and discussions.

REFERENCES

Amblard M, Burch R, Southward BWL (2000). A study of the mechanism of selective conversion of ammonia to nitrogen on Ni/γ-Al_2O_3 under strongly oxidizing conditions. Cataly. Today, 59: 365-371.

Biausque G, Schuurman Y (2010). The reaction mechanism of the high temperature ammonia oxidation to nitric oxide over $LaCoO_3$. J. Catal., 276: 306-313.

Birch MBL, Gramig BM, Moomaw WR, Doering OC, Reeling CJ (2011). Why metrics matter: Evaluating policy choices for reactive nitrogen in the Chesapeake Bay watershed. Environ. Sci. Tech., 45: 168-174.

Brüggemann TC, Keil FJ (2009). Theoretical investigation of the mechanism of the selective catalytic oxidation of ammonia on H-form zeolites. J. Phys. Chem. C, 113: 13860-13876.

Choi JH, Park KW, Park IS, Nam WH, Sung YE (2004). Methanol electro-oxidation and direct methanol fuel cell using Pt/Rh and Pt/Ru/Rh alloy catalysts. Electro. Acta, 50: 787-790.

Cui X, Zhou J, Ye Z, Chen H, Li L, Ruan M, Shi J (2010). Selective catalytic oxidation of ammonia to nitrogen over mesoporous CuO/RuO_2 synthesized by co-nanocasting-replication method. J. Catal., 270: 310-317.

Curtin T, Regan FO, Deconinck C, Knűttle N, Hodnett BK (2000). The catalytic oxidation of ammonia: Influence of water and sulfur on selectivity to nitrogen over promoted copper oxide/alumina catalysts. Cataly. Today, 55: 189-195.

Du HY, Wang CH, Hsu HC, Chang ST, Chen US, Yen SC, Chen LC, Shih HC, Chen KH (2008). Controlled platinum nanoparticles uniformly dispersed on nitrogen-doped carbon nanotubes for methanol oxidation. Diamond Related Mater., 17: 535-541.

Galloway JN, Townsend AR, Erisman JW, Bekunda M, Cai Z, Freney JR, Martinelli LA, Seitzinger SP, Sutton MA (2008). Transformation of the nitrogen cycle: Recent trends, questions, and potential solutions, Science, 320: 889-892.

Hu Z, Allen FM, Wan CZ, Heck RM, Steger JJ, Lakis RE, Lyman CE (1998). Performance and structure of Pt-Rh three-way catalysts: Mechanism for Pt/Rh synergism. J. Catal., 174: 13-21.

Hung CM (2007). Wet air oxidation of aqueous ammonia solution catalyzed by bimetallic Pt/Rh nanoparticle catalysts. J. Chin. Inst. Eng., 30: 977-981.

Hung CM (2008). Decomposition kinetics of ammonia in gaseous stream by a nanoscale copper-cerium bimetallic catalyst. J. Hazard. Mater., 150: 53-61.

Hung CM, Lin WB, Ho CL, Shen YH, Hsia SY (2010). Treatment of ammonia by catalytic wet oxidation process over platinum-rhodium bimetallic catalyst in a trickle-bed reactor: Effect of pH. Water Environ. Res., 82: 686-695.

Hung CM (2011a). Fabrication, characterization, and evaluation of the cytotoxicity of platinum-rhodium nanocomposite materials for use in ammonia treatment. Powder Tech., *209*: 29-34.

Hung CM (2011b). Preparation, properties and cytotoxicity assessment of nanosized Pt-Rh composite catalyst for the decomposition of gaseous ammonia. Adv. Mater. Res., 160-162: 1285-1290.

Liang C, Li W, Wei Z, Xin Q, Li C (2000). Catalytic decomposition of ammonia over nitrided MoNx/α-Al_2O_3 and NiMoNy/α-Al_2O_3 catalysts. Indus. Eng. Chem. Res., 39: 3694-3697.

Oliveira RTS, Santos MC, Nascente PAP, Bulhões LOS, Pereira EC (2008). Nanogravimetric and voltammetric studies of a Pt-Rh alloy surface and its behavior for methanol oxidation. Int. J. Elect. Sci., 3: 970-979.

Prasad KV, Chavdhari RV (1994). Activity and selectivity of supported Rh catalysts for oxidative carbonylation of aniline. J. Catal., 145: 204-215.

Schmidt-Szałowski K, Krawczyk K, Petryk J (1998). The properties of cobalt oxide catalyst for ammonia oxidation. Appl. Catal. A: Gen., 175: 147-157.

Scott WW, Leech WD (1927). Catalytic oxidation of ammonia. Indus. Eng. Chem., 19: 170-173.

Stoyanovskii VO, Vedyagin AA, Aleshina GI, Volodin AM, Noskov AS (2009). Characterization of Rh/Al_2O_3 catalysts after calcination at high temperatures under oxidizing conditions by luminescence spectroscopy and catalytic hydrogenolysis. Appl. Catal. B: Environ., 90: 141-146.

Wang W, Padban N, Ye Z, Andersson A, Bjerle I (1999). Kinetic of ammonia decomposition in hot gas cleaning. Indus. Eng. Chem. Res., 38: 4175-4182.

Wu ML, Lai LB (2004). Synthesis of Pt/Ag bimetallic nanoparticles in water-in-oil microemulsions. Colloids Surf. A: Phys. Eng. Aspects, 244: 149-157.

Zhang L, He H (2009). Mechanism of selective catalytic oxidation of ammonia to nitrogen over Ag/Al_2O_3. J. Catal., 268: 18-25.

Zhang S, Zhao Y (2011). Facile preparation of organic nanoparticles by interfacial cross-linking of reversed micelles and template synthesis of subnanometer Au-Pt nanoparticles. Nano, 5: 2637-2646.

Zhang Y, Dore AJ, Ma L, Liu XJ, Ma WQ, Cape JN, Zhang FS (2010). Agricultural ammonia emissions inventory and spatial distribution in the north China plain. Environ. Pollut., 158: 490-501.

Zhang Y, Geddes CD (2010). Metal-enhanced fluorescence from thermally stable rhodium nanodeposits. J. Mater. Chem., 20: 8600-8606.